Synthesis of Trityl Radical-Conjugated Disulfide Biradicals for Measurement of Thiol Concentration

Yangping Liu,[†] Yuguang Song,[†] Antal Rockenbauer,[§] Jian Sun,[†] Craig Hemann,[†] Frederick A. Villamena,[†,‡] and Jay L. Zweier*[,†]

[†]Center for Biomedical EPR Spectroscopy and Imaging, The Davis Heart and Lung Research Institute, the Division of Cardiovascular Medicine, Department of Internal Medicine, and [‡]Department of Pharmacology, College of Medicine, The Ohio State University, Columbus, Ohio 43210, United States

[§]Chemical Research Center, Institute of Structural Chemistry, P.O. Box 17, H-1525 Budapest, Hungary

S *Supporting Information*

ABSTRACT: Measurement of thiol concentrations is of great importance for characterizing their critical role in normal metabolism and disease. Low-frequency electron paramagnetic resonance (EPR) spectroscopy and imaging, coupled with the use of exogenous paramagnetic probes, have been indispensable techniques for the in vivo measurement of various physiological parameters owing to the specificity, noninvasiveness and good depth of magnetic field penetration in animal tissues. However, in vivo detection of thiol levels by EPR spectroscopy and imaging is limited due to the need for improved probes. We report the first synthesis of trityl radical-conjugated disulfide biradicals (TSSN and TSST) as paramagnetic thiol probes. The use of trityl radicals in the construction of these biradicals greatly facilitates thiol measurement by EPR spectroscopy since trityls have extraordinary stability in living tissues with a single narrow EPR line that enables high sensitivity and resolution for in vivo EPR spectroscopy and imaging. Both biradicals exhibit broad characteristic EPR spectra at room temperature because of their intramolecular spin—spin interaction. Reaction of these biradicals with thiol compounds such as glutathione (GSH) and cysteine results in the formation of trityl monoradicals which exhibit high spectral sensitivity to oxygen. The moderately slow reaction between the biradicals and GSH ($k_2 \sim 0.3\ M^{-1}\ s^{-1}$ for TSSN and $0.2\ M^{-1}\ s^{-1}$ for TSST) allows for in vivo measurement of GSH concentration without altering the redox environment in biological systems. The GSH concentration in rat liver was determined to be 3.49 ± 0.14 mM by TSSN and 3.67 ± 0.24 mM by TSST, consistent with the value (3.71 ± 0.09 mM) determined by the Ellman's reagent. Thus, these trityl-based thiol probes exhibit unique properties enabling measurement of thiols in biological systems and should be of great value for monitoring redox metabolism.
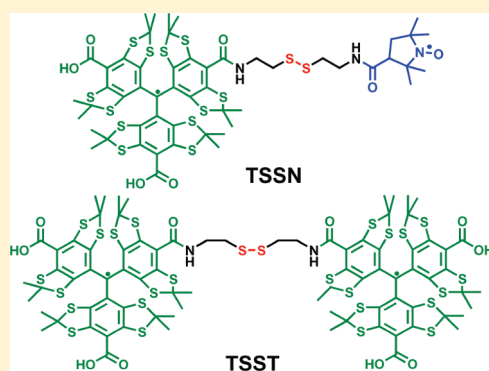
INTRODUCTION

Thiols play an important role in biochemistry, both as components of protein structures and as metabolic intermediates. As a principal nonprotein thiol compound, reduced glutathione (GSH) plays an important role in many biological processes such as transport, protein synthesis, catabolism, and metabolism.[1] GSH can also protect cells against oxidative stress and take part in the detoxification of many xenobiotics. Moreover, the redox state of GSH/glutathione disulfide (GSSG) couple has been considered to be the major intracellular redox buffer and redox regulator.[2] Therefore, techniques that are able to quantify and detect the biological thiols, especially GSH, as well as the related redox status are crucial tools to investigate their roles in various diseases and determine the efficacy of potential therapies.

Many techniques have been developed to measure thiol concentration, including HPLC,[3] electrochemistry,[4,5] and spectrofluorimetry,[6-8] but these methods are mostly limited to in vitro or ex vivo detection due to invasiveness and/or insufficient light penetration into tissues. In the past decades, great progress in low-frequency electron paramagnetic resonance (EPR) instrumentation[9-13] has been achieved which allows in vivo measurement and mapping of different physiological parameters such as oxygen,[12,14-23] redox status,[24-30] pH,[31-34] and reactive oxygen species[35-37] in isolated tissues and living animals. Although there are a variety of endogenous free radicals present in biological systems, they are only present in very low concentrations due to their short half-lives. Thus, exogenous paramagnetic probes with good spectral response to physiological parameters must be introduced into the system under investigation in order to enable EPR detection.

To date, several dinitroxides with a disulfide bond as linker have been developed as EPR thiol probes.[38-40] The thiol—disulfide exchange of the dinitroxides with thiols was
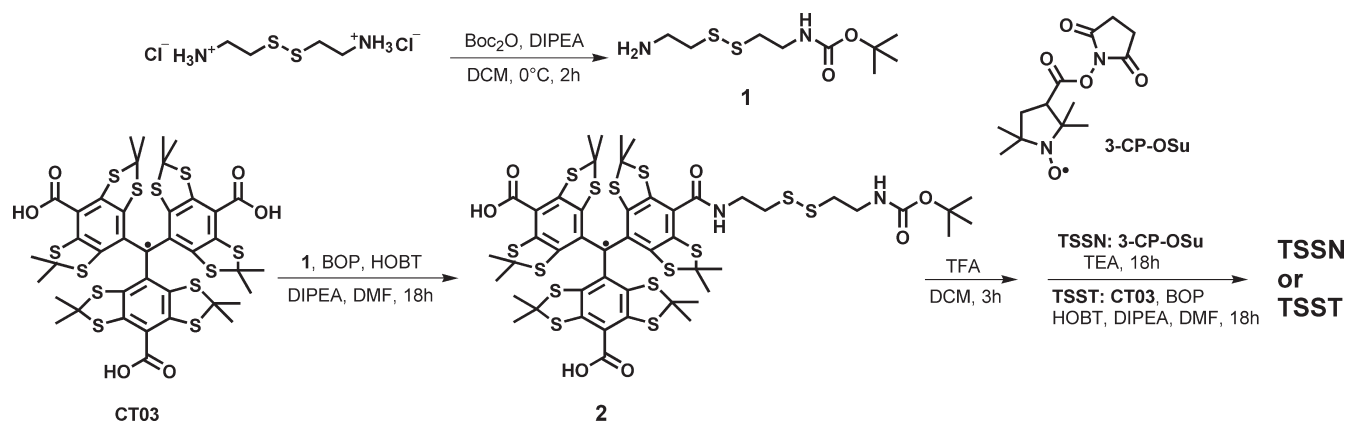
Chart 1. Molecular Structures of Trityl-Conjugated Biradicals (TSSN and TSST) and Trityl Nitroxide Biradicals

TSSN

TSST

CT03, R = OH

TNN14, R =

TN1, R = HN

TN2, R =
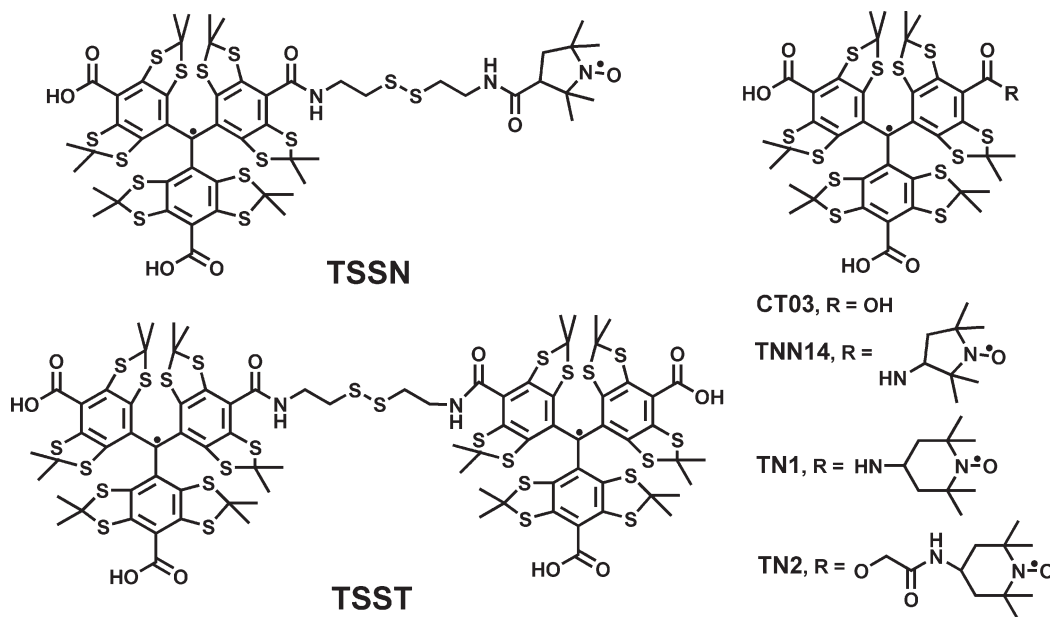
Scheme 1. Synthesis of Trityl-Conjugated Biradicals

followed by EPR to quantitate the thiol (typically GSH) concentrations in blood, plasma, erythrocytes,[39] as well as ovarian xenograft tumors.[40] However, these probes exhibit strong background signals because there are at least two components in their EPR spectra and one of them has a signal similar to that of the nitroxide monoradical at room temperature because of a very weak intramolecular spin—spin interaction ($J \sim 0$ G). In addition, facile bioreduction, a moderately broad EPR triplet, and low oxygen sensitivity limit in vivo applications of the resulting nitroxide monoradical.

Recently, tetrathiatriarylmethyl trityl radicals have received wide attention as EPR probes owing to high biostability and a narrow singlet EPR signal at physiological pH, thereby providing more than 15-fold higher sensitivity and 200-fold improved time resolution for EPRI applications as compared to nitroxides.[41−49] While the field of trityl probe development is still in its infancy, trityl radicals and their derivatives have been utilized to measure extracellular[50] and intracellular[45,51] oxygen levels, superoxide radical anion,[52] pH,[53,54] as well as redox status.[55,56]

In the present study, we report the synthesis of two novel trityl-conjugated biradicals (TSSN and TSST, Chart 1) as thiol probes where the trityl radical (CT03) is linked with the nitroxide radical and another CT03, respectively, through a disulfide bond. These two biradicals show high sensitivity for the measurement of GSH, and the resulting trityl monoradical is well suited as an EPR oximetry probe due to extraordinary stability, narrow line width, and enhanced sensitivity to molecular oxygen. Their application for the measurement of tissue GSH levels was also evaluated.

2. RESULTS AND DISCUSSION

The synthesis of the biradicals TSSN and TSST is shown in Scheme 1. According to the reported method,[57] the monoprotected cystamine (1) was first obtained with a yield of 45% using di-*tert*-butyl dicarbonate in the presence of excess cystamine dihydrochloride. Then, the coupling reaction of compound 1 with the trityl radical CT03 led to the monoprotected cystamine-linked trityl TSS-Boc with a yield of 52%. Finally, the trityl-conjugated
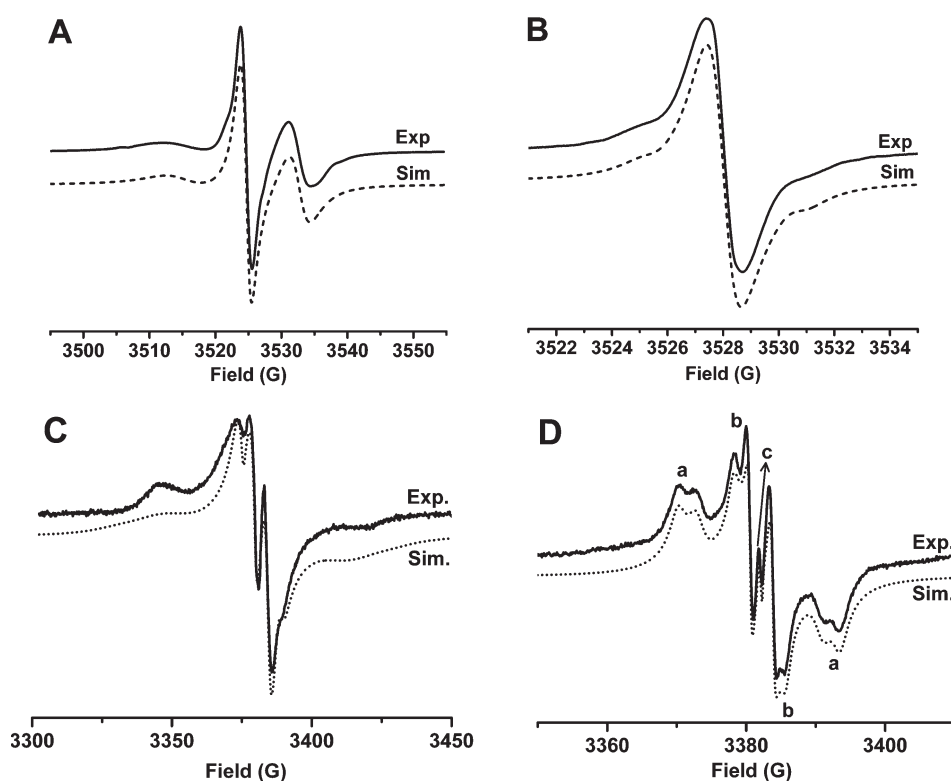
Figure 1. Experimental and simulated EPR spectra of (A) TSSN and (B) TSST in phosphate buffer (PB, pH 7.4, 20 mM) at room temperature and (C) TSSN at 153 K and (D) TSST at 243 K in ethylene glycol/H_2O (1:1, v/v) glass-forming solution. In Figure D, a and b indicate two conformers of TSST and c indicates a trace of trityl monoradical (ca. 0.1%).

biradicals TSSN and TSST were obtained by deprotection of compound **2** using TFA, followed by coupling reactions with 3-CP-OSu[56] for TSSN (65%) or CT03 for TSST (21%) which were characterized by HRMS and IR. The purity of both biradicals was determined by EPR spectroscopy as reported previously[45,56] (96.3 ± 1.2% for TSSN and 94.7 ± 1.8% for TSST) (see the Supporting Information). In addition, HPLC studies were carried out on the biradicals (see the Supporting Information). As shown in Figure S3 (Supporting Information), only one peak (i.e., one component) was observed in the chromatograms of both biradicals, further indicative of their high purity.

The EPR spectrum of TSSN in aqueous solution at ambient temperature is characteristic of a trityl nitroxide biradical with an asymmetric triplet (Figure 1A). The EPR spectral profile of TSSN was not affected in the concentration range of 10−500 μM (Figure S4, Supporting Information), verifying the intramolecular nature of the spin interaction. Computer simulations[58] gave an average J-coupling value of 81.7 G for TSSN. In contrast to the previous trityl nitroxide biradical TNN14 whose EPR triplet features have almost the same line width and amplitude, the low-field first line in the spectrum of TSSN is much weaker and broader due to the long and flexible cystamine linker in TSSN as compared to the short amide bond in TNN14. In the glass-forming solution of ethylene glycol/H_2O (1:1, v/v), the EPR spectrum of TSSN at 153 K (Figure 1C) exhibits the zero-field pattern of the $S = 1$ system with broader lines and wider spectral width compared to the spectrum in Figure 1A. Computer simulation of this spectrum gives rise to two relatively small zero-field splitting (ZFS) parameters: $D = 6.9$ G and $E = 0.8$ G. On the other hand, two components were observed for TSST in

aqueous solution at ambient temperature (Figure 1B). Computer simulations[58] showed that the EPR spectrum of TSST consists of a superposition of a singlet (94.8 ± 0.3%) and a doublet (5.2 ± 0.3%) with a splitting of 5.28 ± 0.02 G. The major singlet has a relatively broad EPR signal with a linewidth of 1.34 G owing to the partially averaged dipolar interaction of two trityl moieties compared to ~0.2 G for CT03 under aerobic conditions. The doublet can be interpreted as the hyperfine interaction with the ^{13}C nuclei in the molecule which was more pronounced at higher temperature (343 K) (see Figure S7, Supporting Information). The concentration-independent EPR profile and singlet/doublet ratio (see Figure S5, Supporting Information) in TSST further ensures the correct assignment of the doublet. The presence of the ^{13}C hyperfine splitting allows the determination of the J-coupling value of TSST by the computer simulation which was estimated to be 40−50 G at 343 K. *Note: because of the large J-coupling, the ^{13}C splittings are reduced by a factor of 2 compared to the splittings in the respective monoradicals* (see Figures S7 and S8, Supporting Information). In the frozen solution of TSST (Figure 1D), superimposed EPR spectra of two conformers were observed with a population of 80.6% for conformer (a) and 19.4% for conformer (b) at 243 K. The ZFS parameters of conformer (a) were estimated by the simulation to be $D = 11.47$ G and $E = 2.06$ G at 243 K, and the corresponding values for conformer (b) are $D = 5.40$ G and $E = 0.71$ G. On the basis of the larger D value of conformer (a), it can be expected that this conformer possesses a twisted geometry with a shorter interspin distances between the two trityl moieties compared to a more planar structure for conformer (b). Interestingly, the population of the two conformers is temperature-dependent
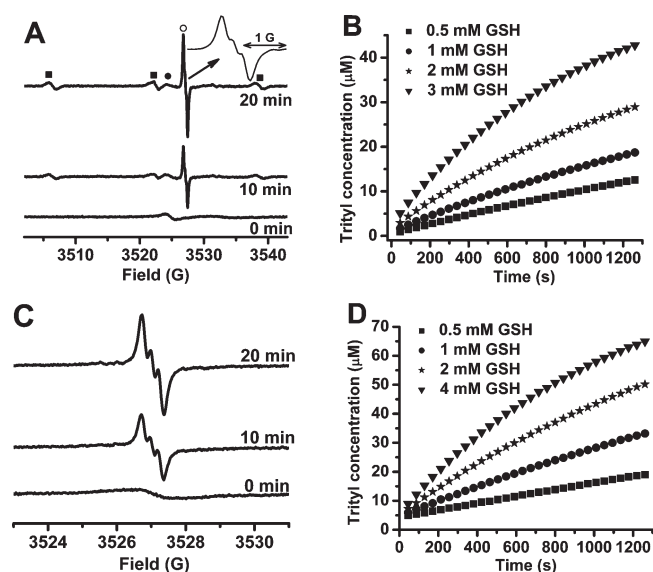
Figure 2. (A) EPR spectra obtained by reaction of TSSN (50 μM) with GSH (2 mM) in PB (50 mM, pH 7.4) at room temperature. EPR signals of ($\bigcirc$) trityl monoradical, ($\blacksquare$) nitroxide monoradical, and ($\bullet$) the biradical TSSN were observed. The inset shows an expanded portion of the spectrum of the trityl monoradical to better visualize its triplet hyperfine structure. Spectra were recorded with 2 mW microwave power, 0.08 G modulation amplitude. (B) Plot of the trityl concentration as a function of time; the trityl monoradical was generated by mixing TSSN (50 μM) with various concentrations of GSH (0.5, 1, 2, and 3 mM). (C) EPR spectra obtained by reaction of TSST (50 μM) with GSH (4 mM) in PB (50 mM, pH 7.4). Spectra were recorded with 1 mW microwave power, 0.05 G modulation amplitude. (D) Plot of the trityl concentration as a function of time. The trityl monoradical was generated by mixing TSST (50 μM) with various concentrations of GSH (0.5, 1, 2, and 4 mM).

(see Table S1, Supporting Information), and conformer (a) has a higher population at lower temperature. This result implies that conformer (a) is the ground-state conformer.

Cleavage of the disulfide bond in the biradicals allows separation of two radical moieties and results in an increase in the EPR signal intensity of the corresponding monoradicals. To test this hypothesis and develop an EPR assay for free thiols, the biradical TSSN was first treated with GSH, and the EPR spectra were recorded as a function of time. As shown in Figure 2A, the reduction of TSSN by GSH leads to the appearance of two new EPR signals: the triplet nitroxide signal with hyperfine splitting constant (hfc) of 16.1 G and line width of 1.2 G and the intense partially overlapped triplet trityl signal with hfc of 0.25 G and line width of 0.19 G under aerobic conditions. The signals of both monoradicals increase with the reaction time while the signal of the biradical decreases. Using TEMPO and CT03 as standards, the nitroxide and trityl concentrations at each time point in Figure 2A were determined to be nearly equivalent. However, owing to the difference in the intrinsic line widths and presence versus absence of triplet hyperfine splitting, respectively, of the nitroxide and trityl monoradicals, the trityl signal is approximately 18-fold stronger than the nitroxide signal, and this ratio remains the same throughout the experiment. The unchanged absorbance at 469 nm is an indicator of the stability of the trityl moiety toward GSH under our experimental conditions (Figure S9, Supporting Information), consistent with our

previous results.[46,52] Figure 2B shows the effect of the GSH concentration on the production of the trityl monoradical. Higher concentrations of GSH led to a faster increase in the signal intensity of the trityl signal and vice versa. According to the data shown in Figure 2B, the second-order rate constant (k_2) for the TSSN reduction by GSH was determined to be 0.33 $\pm$ 0.02 M^{-1} s^{-1} in PB (pH 7.4, 50 mM). A similar k_2 (0.31 $\pm$ 0.03 M^{-1} s^{-1}) was also obtained by monitoring the formation kinetics of the nitroxide (Figure S10, Supporting Information), which is further indicative of the homolytic cleavage of the disulfide bond in TSSN by GSH. The moderately small k_2 value of TSSN with GSH allows in vivo measurement of GSH concentration without change of the redox environment in the systems under investigation.

Comparatively, the reaction of TSST with GSH only resulted in two equivalent trityl monoradicals (Figure 2C). The partially resolved triplet trityl signal was more pronounced than that in the case of TSSN (Figure 2A, inset) since lower EPR scan parameters were used (see the caption in Figure 2). Figure 2D shows the formation kinetics of the trityl monoradicals in the reaction of TSST with various concentrations of GSH. The rate constant for the reaction of TSST with GSH was determined to be 0.19 $\pm$ 0.02 M^{-1} s^{-1} in PB (pH 7.4, 50 mM), which is lower than TSSN ($\sim$0.32 M^{-1} s^{-1}) most likely because of the steric effect of two bulky trityl moieties in TSST. In addition, the rate constants of TSSN (0.42 $\pm$ 0.02 M^{-1} s^{-1}) and TSST (0.35 $\pm$ 0.02 M^{-1} s^{-1}) with cysteine were also determined (Figures S11 and S12, Supporting Information), and both biradicals exhibit higher reactivity toward cysteine as compared to GSH because cysteine is less bulky.

Given that the reduction of nitroxide radicals to the corresponding hydroxylamine is the main factor responsible for their spin quenching in biological systems, the reactivity of these two biradicals toward ascorbate was also evaluated. The reduction of TSSN by ascorbate only resulted in the production of the trityl monoradical (Figure S13, Supporting Information). No nitroxide signal was observed throughout the experiment, further implying that the trityl moiety is stable toward ascorbate, consistent with our previous studies.[55,56] Kinetic studies show that TSSN has a rate constant of 0.29 $\pm$ 0.01 M^{-1} s^{-1} with ascorbate (Figure S14, Supporting Information). This value is close to that of the previous trityl nitroxide biradical TNN14 (0.44 $\pm$ 0.07 M^{-1} s^{-1})[56] but much lower than the values[55] for TN1 (4.11 $\pm$ 0.14 M^{-1} s^{-1}) and TN2 (3.48 $\pm$ 0.09 M^{-1} s^{-1}) due to the use of a more stable pyrrolidinyl nitroxide for the construction of biradicals TNN14 and TSSN compared to the piperidinyl nitroxide for TN1 and TN2. High stability of TSSN toward reductants could be very helpful for its use as a thiol probe. In addition, the reactivity of TSST with ascorbate was also studied. TSST is inert to ascorbate under our experimental conditions as evidenced by no change of the EPR spectrum of TSST (50 μM) in the presence of ascorbate (3 mM) in PB (pH 7.4, 50 mM) (Figure S15, Supporting Information).

In order to explore the potential application of the newly synthesized trityl-conjugated biradicals in biological systems, they were utilized to measure the GSH concentration in fresh rat liver homogenate (RLH). Addition of the RLH to the biradical solutions led to the appearance of trityl and nitroxide (in the case of TSSN) signals. Figure 3 shows plots of trityl and nitroxide monoradical concentrations as a function of time with or without addition of exogenous GSH (0.5 mM). Fitting the trityl formation kinetics from TSST as a monoexponential

process, which is characteristic for its reaction with GSH, yields a value for the GSH concentration of 0.78 ± 0.05 mM in RLH and a corresponding value of 3.67 ± 0.24 mM in liver tissue. Exogenous addition of GSH (0.5 mM) to RLH resulted in an observed GSH concentration of 1.26 ± 0.06 mM with a recovery of 96%. Since in the case of TSSN the trityl monoradicals were generated from cleavage of the disulfide bond by thiols and the bioreduction of the nitroxide moiety, the GSH concentration could not be obtained by fitting the formation kinetics of the trityl monoradicals using a simple monoexponential function. Although the nitroxide moiety in the biradical and nitroxide monoradical can be reduced in this system, the nitroxide
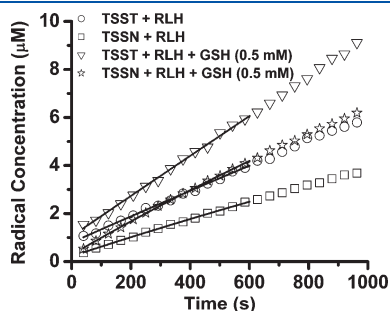

Figure 3. Plot of the monoradical concentrations as a function of time in the fresh rat liver homogenate (RLH). The RLH (40%, v/v) was mixed with the biradical solution (50 μM) in phosphate-buffered saline (PBS, pH 7.4) in the presence or absence of exogenous GSH (0.5 mM). EPR signals of the trityl and nitroxide monoradicals were monitored for TSST and TSSN, respectively, with 2 mW microwave power and 0.08 G modulation amplitude. The trityl and nitroxide concentrations were quantified using CT03 and TEMPO, respectively, as standards. Lines represent the best fit of the initial part of the experimental kinetics to the monoexponents $[\mathrm{M}]/[\mathrm{B}] = 1 - \exp(-k_2[\mathrm{GSH}]t)$ for TSSN and $[\mathrm{M}]/[\mathrm{B}] = 1 - \frac{1}{2}\exp(-k_2[\mathrm{GSH}]t)$ for TSST, where $[\mathrm{M}]$ is the monoradical concentration, $[\mathrm{B}]$ the initial biradical concentration (50 μM), and k_2 the reaction rate constant with GSH. According to the k_2 value of TSSN (0.32 M^{-1} s^{-1}) and TSST (0.19 M^{-1} s^{-1}) at pH 7.4 and 25 °C, the GSH concentrations without exogenous GSH were determined by TSSN to be 0.74 ± 0.03 mM in the RLH with a corresponding value of 3.49 ± 0.14 mM in liver tissue and 0.78 ± 0.05 mM in the RLH with a value of 3.67 ± 0.24 mM in liver tissue by TSST. Exogenous addition of GSH (0.5 mM) in the RLH led to the increased values of 1.21 ± 0.05 and 1.26 ± 0.06 mM in the cases of TSSN and TSST, respectively.

kinetics at the initial part can be approximately considered as a monoexponential process since the nitroxide monoradical has a much lower concentration than TSSN, justifying negligible contribution of the bioreduction of the nitroxide monoradical to the kinetics. Thus, the GSH concentration in the RLH was determined using TSSN to be 0.74 ± 0.03 mM in the RLH with a corresponding value of 3.49 ± 0.14 mM in liver tissue. Exogenous addition of GSH (0.5 mM) to the RLH led to an increased value $(1.21 \pm 0.05$ mM) with a recovery of 94%. Ellman's reagent, which is the most popular reagent for quantitation of thiol concentration in biological systems, was also used to determine the GSH concentration in this system and afforded a very similar value $(0.79 \pm 0.02$ mM) in the RLH and a value of 3.71 ± 0.09 mM in liver tissue.

As we have previously reported,[55,56] the partially overlapped central triplet EPR peaks of the trityl radicals are sensitive to O_2, and the spectral ratio (I_{in}/I_{out}) exhibits enhanced sensitivity toward O_2, especially at low pO_2, relative to the line width. Figure 4A shows the EPR spectrum that was obtained 60 min after reaction of TSSN (50 μM) with GSH (4 mM) under anaerobic conditions. The expanded EPR spectrum (Figure 4B) shows that the trityl monoradical has a well-resolved triplet under anaerobic conditions. Figure 4C shows the oxygen sensitivity of the trityl monoradical(s) resulting from the reduction of TSSN or TSST by GSH. The linearity of I_{in}/I_{out} with the percent oxygen in the range of 0−21% oxygen ensures that these trityl monoradicals can also act as good EPR oximetry probes. Considering that trityl radicals are more sensitive to oxygen than nitroxides, the biradicals TSSN and TSST could find wider application and utility for simultaneous measurement of the GSH concentration and oxygenation than the nitroxide disulfide biradicals.

In conclusion, the newly synthesized trityl-conjugated biradicals TSSN and TSST exhibit characteristic EPR spectral profiles due to their intramolecular spin−spin interactions. Both biradicals are sensitive to GSH and cysteine. Their moderately slow reactions with GSH allow the in vivo measurement of GSH without change of the redox status in the systems. The GSH concentration in rat liver was determined to be 3.49 ± 0.14 mM by TSSN or 3.67 ± 0.24 mM by TSST, consistent with the value $(3.71 \pm 0.09$ mM) in the Ellman's assay. This new probe design has great potential in enabling noninvasive measurement and imaging of thiols in a wide variety of chemical and biological systems.
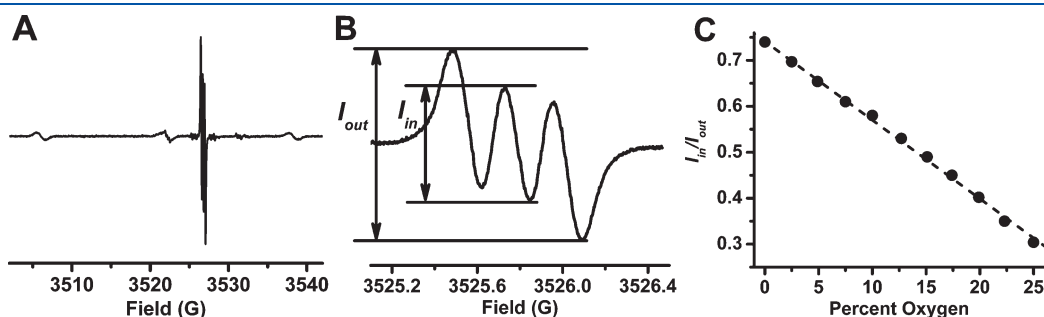

Figure 4. (A) EPR spectrum of the solution containing the trityl and nitroxide monoradicals under anaerobic conditions; spectra were recorded with 0.5 mW microwave power, 0.03 G modulation amplitude, and 50 G sweep width. (B) EPR spectrum of the sample in (A) with a narrow sweep width (1.4 G) to better visualize the triplet hyperfine structure of the trityl monoradical. (C) Plot of I_{in}/I_{out} for the trityl monoradical(s) as a function of O_2 (%). The trityl monoradicals were generated by mixing the biradical TSSN (500 μM) with GSH (3 mM) in NaOH (10 mM) for 60 min since GSH has a higher reactivity toward the disulfide bond at high pH as mentioned previously.[40] The resulting solution was diluted 5-fold using PB (0.1 M, pH 7.4) and used for analysis of oxygen sensitivity.

■ EXPERIMENTAL SECTION

EPR Measurements and Simulations. EPR measurements were carried out on a Bruker EMX X-band EPR spectrometer with an HS resonator at room temperature. General instrument settings were as follows: modulation frequency, 100 kHz; microwave frequency, 9.87 GHz; microwave power, 10 mW for TSSN and nitroxide radicals and 0.5−2 mW for the TSST and trityl monoradicals; modulation amplitude, 1.0 G for TSSN and nitroxide radicals, 0.2 G for TSST and 0.03−0.08 G for the trityl monoradicals; receiver gain, $(1-10.00) \times 10^4$; time constant, 10.24−40.96 ms; sweep time, 10.49−41.94 s.

Simulations were carried out using the EPR simulation program (ROKI\EPR) developed by Prof. Rockenbauer.[58] The fitting routine to determine the J values of the trityl-conjugated biradicals was similar to the method described in our previous studies.[55,56] While TSSN has only one component with a J-coupling value of ∼82 G, two components were observed for TSST. TSST has a superimposed EPR signal consisting of a singlet (94.8 ± 0.3%) and a doublet (5.2 ± 0.3%) with a splitting of 5.28 ± 0.02 G.

EPR spectra in the frozen solution were simulated by assuming anisotropic g- hyperfine and ZF interactions of an $S = 1$ spin system. The principal values of tensors were supposed to be parallel. The strain or mobility effects in the glass were taken into account by a line width tensor. The ZF parameters are more reliable for TSST than for TSSN, since in the latter case the hyperfine interaction can mix the $S = 1$ and $S = 0$ states, which was not included in our computations.

Oxygen Sensitivity. Oxygen sensitivity of the trityl monoradical was evaluated according to our previous method.[55,56] Briefly, 50 μL of the solution containing GSH (3 mM) and TSSN (500 μM) in NaOH (10 mM) was incubated for 60 min at room temperature. Then, the solution was diluted into 250 μL using PB (0.1 M, pH 7.4), transferred into a gas-permeable Teflon tube (i.d. = 0.8 mm), and sealed at both ends. The sealed sample was placed inside a quartz EPR tube with open ends. Nitrogen or N_2/O_2 gas mixture with varying concentrations of O_2 was allowed to diffuse into the EPR tube and, after about 4 min, was changed into another gas mixture. EPR spectra were recorded using the incremental sweep model. The spectral ratio (I_{in}/I_{out}) was calculated from the spectra.

Reaction Kinetics of Trityl-Conjugated Biradicals with GSH. Various concentrations of GSH (0.5, 1, 2, and 3 mM) were added to the solution of the biradical (50 μM) in PB (50 mM, pH 7.4). Incremental EPR spectra were recorded 45 s after mixing. The concentration of the trityl monoradical(s) at each time point was obtained by comparing their doubly integrated signal intensities relative to CT03 as standard. Since the GSH concentration (0.5, 1, 2, and 3 mM) used was in higher excess than the biradical concentration (50 μM), the reaction kinetics of the biradical with GSH is a pseudo-first-order reaction. The plots of the trityl concentrations as a function of time (see the Supporting Information) were fitted with the equation $\ln[(C_0 - C_t)/C_0] = -k_{obs}t$, where C_0 is the initial concentration of the biradical, C_t the trityl monoradical(s) at each time point, and k_{obs} the observed pseudo-first-order rate constant. Considering $k_{obs} = k_2[GSH]$, the approximated second-order rate constant k_2 was finally calculated from the slope of the plot of k_{obs} versus [GSH].

Measurement of GSH Concentration in Rat Liver. On the day of the experiments, rats were sacrificed and rat livers were taken. Rat livers were weighed and cut into small pieces and washed with PBS (pH 7.4) to remove blood. The resulting liver pieces were blotted with paper towels and then transferred to a homogenizer. Then, a 4-fold volume of PBS (pH 7.4) was added to the homogenizer, and the liver pieces were manually ground. The homogenate was centrifuged at 4000 rpm at 4 °C for 15 min, and the resulting supernatant was further ultracentrifuged at 12000 rpm (4 °C) for 60 min using a membrane filter with a MW cutoff of 3000 Da. The filtrate was collected for EPR analysis, and the GSH

concentration was determined by TSSN and TSST to be 0.74 ± 0.03 mM in the fresh rat liver homogenate with a corresponding value of 3.49 ± 0.14 mM in liver tissue and 0.78 ± 0.05 mM with a corresponding value of 3.67 ± 0.24 mM in liver tissue, respectively. Exogenous addition of GSH (0.5 mM) to RLH resulted in a recovery of 96% and 94% in the cases of TSST and TSSN, respectively. In order to further verify the validity of the present method, Ellman's reagent was also used, and the GSH concentration was determined to 0.79 ± 0.02 mM in the RLH and a value of 3.71 ± 0.09 mM in rat liver, consistent with the values obtained using the biradicals.

Synthesis. *TSS-Boc.* To the solution of CT-03 (200 mg, 0.2 mmol), 1-hydroxybenzotriazole (HOBt, 81 mg, 0.6 mmol), and (benzotriazol-1-yloxy)tris(dimethylamino)phosphonium hexafluorophosphate (BOP, 93 mg, 0.21 mmol) in dry DMF (20 mL) was added N,N-diisopropyl-ethylamine (DIPEA, 200 μL) under N_2. The reaction mixture was stirred at room temperature for 20 min, and then the monoprotected cystamine (**1**)[57] (53 mg, 0.21 mmol) in 8 mL of DMF was added dropwise. The resulting mixture was continuously stirred for 18 h at room temperature. Solvent was removed under vacuum, and the residue was dissolved in PB (0.1 M, pH 7.4) and purified by column chromatography on reversed-phase C-18 using water followed by 0−15% acetonitrile in water as eluants to give the compound **2** as a green solid (128 mg, 52%): IR (cm^{-1}, neat) 3340.7, 2971.9, 2922.8, 2863.2, 1691.4, 1662.6, 1514.4, 1492.2, 1452.3, 1432.4, 1366.1, 1231.0, 1167.3, 1149.6, 1112.3, 1044.0, 886.1, 722.5; HRMS [MALDI-TOF, dihydroxybenzoic acid (DHB) as the matrix] m/z calcd for $C_{49}H_{57}N_2O_7S_{14}{}^{\bullet}$ ([M]$^+$) 1233.026, found 1233.016; calcd for $C_{49}H_{57}N_2NaO_7S_{14}{}^{\bullet}$ ([M+Na]$^+$) 1256.015, found 1256.023.

TSSN. To a suspension of TSS-Boc (50 mg, 40.5 μmol) in DCM (2 mL) was added TFA (2 mL). The reaction mixture was stirred for 3 h at room temperature and evaporated to dryness under vacuum. The residue was redissolved in 5 mL of DMF, and DIPEA (200 μL) and 3-CP-OSu[56] (12.6 mg, 44.6 μmol) were then added. The resulting reaction mixture was continuously stirred for 18 h at room temperature. Solvent was removed under vacuum, and the residue was dissolved in PB (0.1 M, pH 7.4) and purified by column chromatography on reversed-phase C-18 using water followed by 0−15% acetonitrile in water as eluant to give TSSN as a green solid (34 mg, 65%). Purity: 96.3 ± 1.2% versus 4-hydroxy-2,2,6,6-tetramethylpiperidine-N-oxyl (TEMPOL) determined as previously reported:[45,56] IR (cm^{-1}, neat) 3325.2, 2969.1, 2923.4, 2857.1, 1698.1, 1658.3, 1525.9, 1492.5, 1453.5, 1383.8, 1365.8, 1232.4, 1168.1, 1149.3, 1111.9, 1042.9, 886.1, 721.4; HRMS (MALDI-TOF, DHB as the matrix) m/z calcd for $C_{53}H_{63}N_3O_7S_{14}{}^{\bullet\bullet}$ ([M]$^+$) 1301.076, found 1300.967; calcd for $C_{53}H_{63}N_3NaO_7S_{14}{}^{\bullet\bullet}$ ([M + Na]$^+$) 1324.065, found 1323.975; calcd for $C_{53}H_{63}KN_3O_7S_{14}{}^{\bullet\bullet}$ ([M + K]$^+$) 1340.039, found 1339.944; HPLC (reversed phase) retention time, 22.6 min.

TSST. To a suspension of TSS-Boc (50 mg, 40.5 μmol) in DCM (2 mL) was added TFA (2 mL). The reaction mixture was stirred for 3 h at room temperature and evaporated to dryness under vacuum. The residue was redissolved in 5 mL of DMF and added dropwise to the solution obtained by mixing CT-03 (44 mg, 44 μmol), HOBt (17.8 mg, 0.13 mmol), BOP (20.4 mg, 46 μmol), and DIPEA (90 μL) in dry DMF (10 mL). The resulting reaction mixture was continuously stirred for 18 h at room temperature. Solvent was removed under vacuum, and the residue was dissolved in PB (0.1 M, pH 7.4) and purified by column chromatography on reversed-phase C-18 using water followed by 0−30% acetonitrile in water as eluants to give TSST as a green solid (18 mg, 21%). Purity: 94.7 ± 1.8% versus TEMPOL determined as previously reported:[45,56] IR (cm^{-1}, neat) 3346.1, 2966.1, 2918.1, 2863.6, 1699.4, 1665.6, 1517.2, 1492.3, 1452.5, 1365.8, 1231.1, 1167.7, 1149.2, 1111.9, 1043.3, 886.1, 722.3; HRMS (MALDI-TOF, DHB as the matrix) m/z calcd for $C_{84}H_{86}N_2O_{10}S_{26}{}^{\bullet\bullet}$ ([M]$^+$) 2113.902, found 2113.967; calcd for $C_{84}H_{86}N_2NaO_{10}S_{26}{}^{\bullet\bullet}$ ([M + Na]$^+$) 2136.892, found 2137.061; HPLC (reversed-phase) retention time, 27.6 min.

■ ASSOCIATED CONTENT

ⓈSupporting Information. Purity analysis, EPR studies and simulation, IR and HRMS spectra, HPLC chromatograms, and kinetic studies. This material is available free of charge via the Internet at http://pubs.acs.org.

■ AUTHOR INFORMATION

Corresponding Author

*Email: jay.zweier@osumc.edu.

■ REFERENCES

(1) Meister, A.; Anderson, M. E. *Annu. Rev. Biochem.* **1983**, *52*, 711–760.

(2) Schafer, F. Q.; Buettner, G. R. *Free Radical Biol. Med.* **2001**, *30*, 1191–1212.

(3) Katrusiak, A. E.; Paterson, P. G.; Kamencic, H.; Shoker, A.; Lyon, A. W. *J. Chromatogr. B* **2001**, *758*, 207–212.

(4) White, P. C.; Lawrence, N. S.; Davis, J.; Compton, R. G. *Electroanalysis* **2002**, *14*, 89–98.

(5) Wang, W.; Li, L.; Liu, S. F.; Ma, C. P.; Zhang, S. S. *J. Am. Chem. Soc.* **2008**, *130*, 10846–+.

(6) Chen, X.; Zhou, Y.; Peng, X. J.; Yoon, J. *Chem. Soc. Rev.* **2010**, *39*, 2120–2135.

(7) Lee, J. H.; Lim, C. S.; Tian, Y. S.; Han, J. H.; Cho, B. R. *J. Am. Chem. Soc.* **2010**, *132*, 1216–+.

(8) Shao, N.; Jin, J. Y.; Wang, H.; Zheng, J.; Yang, R. H.; Chan, W. H.; Abliz, Z. *J. Am. Chem. Soc.* **2010**, *132*, 725–736.

(9) Kuppusamy, P.; Chzhan, M.; Samouilov, A.; Wang, P.; Zweier, J. L. *J. Magn. Reson. Ser. B* **1995**, *107*, 116–125.

(10) Nicholson, I.; Robb, F. J. L.; McCallum, S. J.; Koptioug, A.; Lurie, D. J. *Phys. Med. Biol.* **1998**, *43*, 1851–1855.

(11) Kuppusamy, P.; Shankar, R. A.; Zweier, J. L. *Phys. Med. Biol.* **1998**, *43*, 1837–1844.

(12) Elas, M.; Williams, B. B.; Parasca, A.; Mailer, C.; Pelizzari, C. A.; Lewis, M. A.; River, J. N.; Karczmar, G. S.; Barth, E. D.; Halpern, H. J. *Magn. Reson. Med.* **2003**, *49*, 682–691.

(13) Samouilov, A.; Caia, G. L.; Kesselring, E.; Petryakov, S.; Wasowicz, T.; Zweier, J. L. *Magn. Reson. Med.* **2007**, *58*, 156–166.

(14) Grucker, D. *Prog. Nucl. Magn. Reson. Spectrosc.* **2000**, *36*, 241–270.

(15) He, G.; Shankar, R. A.; Chzhan, M.; Samouilov, A.; Kuppusamy, P.; Zweier, J. L. *Proc. Natl. Acad. Sci. U.S.A.* **1999**, *96*, 4586–4591.

(16) James, P. E.; Jackson, S. K.; Grinberg, O. Y.; Swartz, H. M. *Free Radical Biol. Med.* **1995**, *18*, 641–647.

(17) Swartz, H. M.; Liu, K. J.; Goda, F.; Walczak, T. *Magn. Reson. Med.* **1994**, *31*, 229–232.

(18) Zweier, J. L.; Chzhan, M.; Ewert, U.; Schneider, G.; Kuppusamy, P. *J. Magn. Reson. Ser. B* **1994**, *105*, 52–57.

(19) Zweier, J. L.; He, G. L.; Samouilov, A.; Kuppusamy, P. *Oxygen Transp. Tissue xxiv* **2003**, *530*, 123–131.

(20) Elas, M.; Ahn, K. H.; Parasca, A.; Barth, E. D.; Lee, D.; Haney, C.; Halpern, H. J. *Clin. Cancer Res.* **2006**, *12*, 4209–4217.

(21) Gallez, B.; Baudelet, C.; Jordan, B. F. *NMR Biomed.* **2004**, *17*, 240–262.

(22) Gallez, B.; Mader, K. *Free Radical Biol. Med.* **2000**, *29*, 1078–1084.

(23) Halpern, H. J.; Yu, C.; Peric, M.; Barth, E.; Grdina, D. J.; Teicher, B. A. *Proc. Natl. Acad. Sci. U.S.A.* **1994**, *91*, 13047–13051.

(24) He, G. L.; Kutala, V. K.; Kuppusamy, P.; Zweier, J. L. *Free Radical Biol. Med.* **2004**, *36*, 665–672.

(25) Hyodo, F.; Chuang, K. H.; Goloshevsky, A. G.; Sulima, A.; Griffiths, G. L.; Mitchell, J. B.; Koretsky, A. P.; Krishna, M. C. *J. Cereb. Blood Flow Metab.* **2008**, *28*, 1165–1174.

(26) Ilangovan, G.; Li, H. Q.; Zweier, J. L.; Krishna, M. C.; Mitchell, J. B.; Kuppusamy, P. *Magn. Reson. Med.* **2002**, *48*, 723–730.

(27) Ilangovan, G.; Li, H. Q.; Zweier, J. L.; Kuppusamy, P. *Mol. Cell. Biochem.* **2002**, *234*, 393–398.

(28) Kuppusamy, P.; Li, H. Q.; Ilangovan, G.; Cardounel, A. J.; Zweier, J. L.; Yamada, K.; Krishna, M. C.; Mitchell, J. B. *Cancer Res.* **2002**, *62*, 307–312.

(29) Swartz, H. M.; Khan, N.; Khramtsov, V. V. *Antioxid. Redox Signal* **2007**, *9*, 1757–1771.

(30) Yamada, K. I.; Kuppusamy, P.; English, S.; Yoo, J.; Irie, A.; Subramanian, S.; Mitchell, J. B.; Krishna, M. C. *Acta Radiol.* **2002**, *43*, 433–440.

(31) Gallez, B.; Mader, K.; Swartz, H. M. *Magn. Reson. Med.* **1996**, *36*, 694–697.

(32) Khramtsov, V. V.; Grigor'ev, I. A.; Foster, M. A.; Lurie, D. J. *Antioxid. Redox Signal* **2004**, *6*, 667–676.

(33) Khramtsov, V. V. *Curr. Org. Chem.* **2005**, *9*, 909–923.

(34) Foster, M. A.; Grigor'ev, I. A.; Lurie, D. J.; Khramtsov, V. V.; McCallum, S.; Panagiotelis, I.; Hutchison, J. M. S.; Koptioug, A.; Nicholson, I. *Magn. Reson. Med.* **2003**, *49*, 558–567.

(35) Ui, I.; Okajo, A.; Endo, K.; Utsumi, H.; Matsumoto, K. *Free Radical Biol. Med.* **2004**, *37*, 2012–2017.

(36) Takeshita, K.; Fujii, K.; Anzai, K.; Ozawa, T. *Free Radical Biol. Med.* **2004**, *36*, 1134–1143.

(37) Halpern, H. J.; Yu, C.; Barth, E.; Peric, M.; Rosen, G. M. *Proc. Natl. Acad. Sci. U.S.A.* **1995**, *92*, 796–800.

(38) Khramtsov, V. V.; Yelinova, V. I.; Weiner, L. M.; Berezina, T. A.; Martin, V. V.; Volodarsky, L. B. *Anal. Biochem.* **1989**, *182*, 58–63.

(39) Khramtsov, V. V.; Yelinova, V. I.; Glazachev, Y. I.; Reznikov, V. A.; Zimmer, G. *J. Biochem. Biophys. Methods* **1997**, *35*, 115–128.

(40) Roshchupkina, G. I.; Bobko, A. A.; Bratasz, A.; Reznikov, V. A.; Kuppusamy, P.; Khramtsov, V. V. *Free Radical Biol. Med.* **2008**, *45*, 312–320.

(41) Ardenkjaer-Larsen, J. H.; Laursen, I.; Leunbach, I.; Ehnholm, G.; Wistrand, L. G.; Petersson, J. S.; Golman, K. *J. Magn. Reson.* **1998**, *133*, 1–12.

(42) Reddy, T. J.; Iwama, T.; Halpern, H. J.; Rawal, V. H. *J. Org. Chem.* **2002**, *67*, 4635–4639.

(43) Xia, S. J.; Villamena, F. A.; Hadad, C. M.; Kuppusamy, P.; Li, Y. B.; Zhu, H.; Zweier, J. L. *J. Org. Chem.* **2006**, *71*, 7268–7279.

(44) Dhimitruka, I.; Velayutham, M.; Bobko, A. A.; Khramtsov, V. V.; Villamena, F. A.; Hadad, C. M.; Zweier, J. L. *Bioorg. Med. Chem. Lett.* **2007**, *17*, 6801–6805.

(45) Liu, Y.; Villamena, F. A.; Sun, J.; Xu, Y.; Dhimitruka, I.; Zweier, J. L. *J. Org. Chem.* **2008**, *73*, 1490–1497.

(46) Liu, Y.; Villamena, F. A.; Zweier, J. L. *Chem. Commun* **2008**, 4336–4338.

(47) Bobko, A. A.; Dhimitruka, I.; Eubank, T. D.; Marsh, C. B.; Zweier, J. L.; Khramtsov, V. V. *Free Radical Biol. Med.* **2009**, *47*, 654–658.

(48) Dhimitruka, I.; Grigorieva, O.; Zweier, J. L.; Khramtsov, V. V. *Bioorg. Med. Chem. Lett.* **2010**, *132*, 3946–3949.

(49) Driesschaert, B.; Charlier, N.; Gallez, B.; Marchand-Brynaert, J. *Bioorg. Med. Chem. Lett.* **2008**, *18*, 4291–4293.

(50) Kutala, V. K.; Parinandi, N. L.; Pandian, R. P.; Kuppusamy, P. *Antioxid. Redox Signal* **2004**, *6*, 597–603.

(51) Liu, Y. P.; Villamena, F. A.; Sun, J.; Wang, T. Y.; Zweier, J. L. *Free Radical Biol. Med.* **2009**, *46*, 876–883.

(52) Rizzi, C.; Samouilov, A.; Kutala, V. K.; Parinandi, N. L.; Zweier, J. L.; Kuppusamy, P. *Free Radical Biol. Med.* **2003**, *35*, 1608–1618.

(53) Bobko, A. A.; Dhimitruka, I.; Zweier, J. L.; Khramtsov, V. V. *J. Am. Chem. Soc.* **2007**, *129*, 7240–7241.

(54) Dhimitruka, I.; Bobko, A. A.; Hadad, C. M.; Zweier, J. L.; Khramtsov, V. V. *J. Am. Chem. Soc.* **2008**, *130*, 10780–10787.

(55) Liu, Y. P.; Villamena, F. A.; Rockenbauer, A.; Zweier, J. L. *Chem. Commun* **2010**, *46*, 628–630.

(56) Liu, Y. P.; Villamena, F. A.; Song, Y. G.; Sun, J.; Rockenbauer, A.; Zweier, J. L. *J. Org. Chem.* **2010**, *75*, 7796–7802.

(57) Niu, H.; Liu, Z. H.; Fu, L.; Shi, F.; Ma, H. W.; Ozaki, Y.; Zhang, X. *Langmuir* **2008**, *24*, 11988–11994.

(58) Rockenbauer, A.; Korecz, L. *Appl. Magn. Reson.* **1996**, *10*, 29–43.